ISBN: 978-3-95450-247-9 ISSN: 2673-5490 doi: 10.18429/JACoW-IPAC2024-MOPS82

DISCOVERING TRANSIENT MODELS OF EMITTANCE GROWTH VIA MODE INTERACTION OF PHASE SPACE NONUNIFORMITIES *

L. A. Pocher†, T. M. Antonsen Jr., L. Dovlatyan, I. Haber, P. G. O'Shea
University of Maryland, College Park, MD, USA

Abstract

One of the Grand Challenges in beam physics is development of virtual particle accelerators for beam prediction. Virtual accelerators rely on efficient and effective methodologies grounded in theory, simulation, and experiment. We address one sample methodology, extending the understanding and the control of deleterious effects, for example, emittance growth. We employ the application of the Sparse Identification of Nonlinear Dynamical systems algorithm—previously presented at NAPAC'22 [1] and IPAC'23 [2]—to identify emittance growth dynamics caused by nonuniform, empirical distributions in phase space in a linear, uniform focusing channel. To gain further understanding of the evolution of emittance growth as the beam's distribution approaches steady state, we compare our results to theoretical predictions describing the final state emittance growth due to collective and N-body mode interaction of space charge nonuniformities as a function of free-energy and space-charge intensity.

MOTIVATION

Nagaitsev *et al.* [3] have enumerated four Grand Challenges enabling future Department of Energy (DOE) High Energy Physics (HEP) programs. Grand Challenge #4 Beam Prediction poses the question: "How do we develop predictive virtual particle accelerators"?

In our prior work [1, 2] we operated underneath the umbrella of this Grand Challenge and were able to elucidate analytic expressions governing beam centroid evolution in an electron ring and moment deviations in a flat to round setup. Our aim is to speed up commissioning and design studies of accelerators by uncovering underlying physics in virtual and real accelerators. Our approach was to apply an existing method from the data-driven, nonlinear dynamics community called *S*parse *I*dentification of *N*onlinear *D*ynamics (SINDy) [4, 5] to uncover physics in problems that can't be solved analytically.

In our current work, we are studying the modal dynamics of the eigenfunctions for a nonuniform beam injected into uniform focusing channel. This work is building on work done by Gluckstern who derived the eigenfunctions to the linearized Boltmann and Poisson equation [6], Lund's work in warm fluid equilibria which also examined and enumerated Gluckstern's eigenfunctions [7]. In addition, to this scholarship, other work in a similar vein has been done by Hofmann [8, 9], Lund [10–12], and Carlsten [13]. This work is also motivated by the Fermi-Pasta-Ulam-Tsingou problem [14] that examined ergodicty and modal interaction in a chain of coupled, nonlinear oscillators. The beam dynamics present within this paper are somewhat similar, as in as we turn up the nonlinear interaction ($1/r^2$) between particles by increasing the space charge the nonlinear particle interaction increases. Key differences are that their oscillators interacted only with nearest neighbors and couldn't force themselves past each other. Our "oscillators" are all the particles in the beam and our modes are not a Fourier transform of the motion of all the particles.

* Work supported by US DOE-HEP grants: DE-SC0010301 and DE-SC0022009.
† lpocher@umd.edu

APPROACH

Our approach is to inject a matched beam into a uniform focusing channel—see Fig. 1(a)—in a first principle simulation (Warp [15]) initialized with one of three initial velocity distributions with(out) a configuration space (x, y) perturbation to observe modal dynamics. The characteristic axial length was set to 1.0 such that calculated phase advances were calculated per axial unit length.

These simulations had 4 million macroparticles, transverse simulation resolution of $N_x = N_y = 512$, a pipe radius bounding the simulation of $r_{\text{pipe}} = 1.3$ cm, and axial step size dz of 1 cm. These simulations were convergence tested in both the axial step size resolution and the transverse resolution. An initial beam size of 2.5 mm was injected into the uniform focusing channel whose electric field gradient $\partial E_r/\partial r = k_E$ was set to an initial value 30.45 kV/m^2 for a zero current simulation. The dimensionless variable $\tilde{r} = r/r_b$ is used for plotting purposes. This potential gives rise to a linear restoring force, $F = -qk_E r$ direction indicated by the green arrows, inducing simple harmonic motion of a single (or N non interacting) charged particle interacting with this potential. We increased the electric field gradient, increasing the undepressed phase advance per axial unit length σ_0, in higher current simulations to keep the same value for depressed phase advance per axial unit length σ.

Three candidate $f_0(v)$, Fig. 1(b), (KV, Parabolic [PL], and Semigaussian [SG]) were selected based on them being stationary solutions to the Boltzmann equation (KV), a warm fluid equations (PL) [7], or neither (SG) to investigate thermalization timescales and dynamics.

To match the beam we estimated a beam envelope from the asymmetric beam envelope equation

$$R'' + \underbrace{\frac{q}{m\gamma^3\beta^2c^2}\,k_E}_{\sigma_0^2\ \text{focusing}}\,R - \underbrace{\frac{K}{R} - \frac{\varepsilon^2}{R^3}}_{\text{defocusing}} = 0 \qquad (1)$$

ISBN: 978-3-95450-247-9 ISSN: 2673-5490 doi: 10.18429/JACoW-IPAC2024-MOPS82

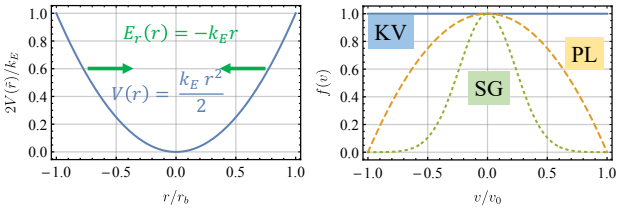

(a) (b)

Figure 1: (a) Electrostatic potential $V(\tilde{r})$, blue line, that the beam interacts with in the uniform focusing channel. (b) Initial velocity distributions used in simulation: blue solid is KV; yellow dashed is the PL distribution; and the green dotted is the SG distribution.

with R being twice the statistical root mean square (rms) horizontal/vertical beam size, $R = 2x_{\rm rms}$, q particle charge, γ the relativistic factor, β the dimensionless beam velocity $\beta = v/c$, c the speed of light, m the particle mass, K the beam perveance, ε the beam's rms total emittance, and σ_0 the undepressed phase advance per axial unit length. An envelope code was iterated to actually obtain a matched beam radius.

Table 1 shows a table of simulations performed with various amounts of space charge. As the space charge is increased the nonlinear interaction between particles in the beam increases. Case (a) simulations are emittance dominated simulations with not nonlinear interaction between particles in the beam, while case (d) simulations are space charge dominated beams. The intensity parameter $\chi = 1 - \sigma^2/\sigma_0^2$ [16] is a dimensionless measure of how much space charge dominates beam dynamics. For $\chi = 0$ the beam is emittance dominated, while for $\chi \to 1$ beams become space charge dominated.

Table 1: Simulation Cases

Case	k_E [kV/m^2]	I [mA]	σ/σ_0	χ
(a)	30.45	0.0	1.00	0.0
(b)	35.37	0.1	0.92	0.13
(c)	55.05	0.5	0.74	0.44
(d)	276.5	5.0	0.33	0.88

Beam Eigenfunctions

The linearized, axisymetric Boltmann and Poisson equations may be shown to have eigenfunctions for the particle number density $n(r)$ that are composed of Legendre Polynomials [6, 7]. The particle number density $n(r)$ can be decomposed into the following form

$$n(r) = \sum \hat{c}_n P_n \left(1 - 2\,(r/r_b)^2\right) \qquad (2)$$

with P_n being the n'th order Legendre polynomials whose argument has been remapped from $x \in [-1, 1]$ to $r \in [r_b, 0.0]$ where r_b is the beam edge[1], $\hat{c}_n$ is the modal amplitude, and $n(r) = N(r)/r$ where $N(r)$ is the physical particle number at that radial location in the beam. In this paper we study the modal amplitude dynamics, $\hat{c}_n(z)$, of these first 6 modes.

The coefficients $\hat{c}_n$ of these eigenfunctions are evaluated from

$$\hat{c}_n = \frac{2n+1}{2} \int_0^{r_b} dr\, w(r)\, P_n \left[1 - 2\left(\frac{r}{r_b}\right)^2\right] n(r) \qquad (3)$$

with n being mode order, $w(r) = 4r/r_b^2$ the orthogonality weighting function for P_n, and $n(r)$ the particle number density.

Candidate Perturbations

We examined five different candidate perturbations δn in Fig. 2(a): a heaviside function $\theta[(1-r)/10]$, an offset, negative parabolic $1-r^2$, an offset, positive parabolic, a Gaussian e^{-10r^2}, and a Maxwell-Boltzmann $10r^2e^{-10r^2}$. We chose the Gaussian δn as it had the highest fidelity reconstructed with the proposed Gluckstern [6, 7] eigenfunctions, see Fig. 2(b).

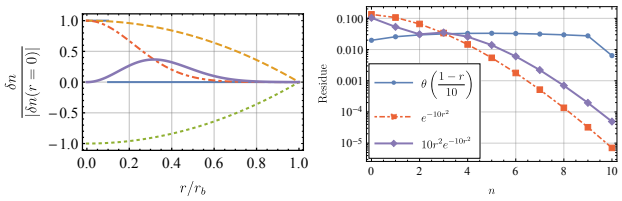

(a) (b)

Figure 2: (a) candidate perturbations $\delta n(\tilde{r})$. The solid blue line is $\theta\,[(1-\tilde{r})\,/10]$, the dashed yellow is $1-\tilde{r}^2$, dotted green $\tilde{r}^2-1$, red dot-dashed $e^{-10\tilde{r}^2}$, and thick purple $10\tilde{r}^2e^{-10\tilde{r}^2}$. The horizontal axis is dimensionless beam radius and the vertical is the dimensionless perturbation divided by their absolute value at $\tilde{r} = 0$. (b) residue of the candidate perturbations with the horizontal axis being the mode number for the reconstructed δn and the vertical axis the residue.

To effect the perturbation in our simulation we took a random 10% of the beam—400,000 particles—and redistributed them randomly into a Gaussian distribution with an angle taken from the uniform $\theta \in [0, 2\pi)$ distribution and dimensionless radial variable $\tilde{r} = r/r_b$ taken from a uniform distribution for x between e^{-10} (upper bound for radius because of -log argument) and 1.0 (lower bound) and then inserted into the following function $\tilde{r} = \sqrt{-2\sigma^2 * \log(x)}$ to obtain bounded Gaussian filling that is truncated at the beam edge with $\sigma^2 = 0.05^2$.

[1] This remapping has implication for the weighting function that maintains the Legendre polynomial orthonormality over the range $r \in [r_b, 0.0]$

[2] This σ^2 is variance of the Gaussian perturbation, not σ the depressed phase advance.

ISBN: 978-3-95450-247-9 ISSN: 2673-5490 doi: 10.18429/JACoW-IPAC2024-MOPS82

RESULTS

A total of 24 different simulations with(out) perturbations with four cases of space charge and three different initial velocity distributions were performed. Shown here are the results for 8 of those simulations with the Gaussian perturbations in configuration space and the KV and the PL initial $f_0(v)$ distributions. The SG initial distribution has slightly faster rise and fall times for certain parts of the modal dynamics for zero space charge, but aside from that show no difference to the PL case and as such are not shown here. The dynamics of the modal coefficients without a perturbation show a marked difference, but are not reported in this paper.

Particle Number Density

Figures 3(a) to 3(d) and 4(a) to 4(d) shows the normalized particle number density $n(\tilde{r}, \tilde{z})$ plotted with the blue corresponding to minimum particle number density and yellow maximum particle number density. These are shown for increasing amounts of space charged $I \in [0.0, 0.1, 0.5, 5]$ mA (σ/σ_0=[1.0, 0.92, 0.74, 0.33], respectively).

For zero space charge, Figs. 3(a) and 4(a) the perturbation reoccurs, a Poincaré recurrence, every half betatron period. As we increase space charge, other feature dynamics are observed in Figs. 3(b), 3(c), 4(b) and 4(c) with the increased amount of space charged creating a thermalization timescale and thus making the beam approach another equilibrium. For the space charge dominated beam, the equilibration timescale is almost instantaneous with either broadband structure observed in the KV beam or what appears to be a limit cycle for the PL beam.

The initial velocity distribution has no impact on the initial configuration space, but as the beam propagates down the lattice the modal dynamics are accelerated and equilibrium via thermalization of the space charge nonuniformintiy is accelerated.

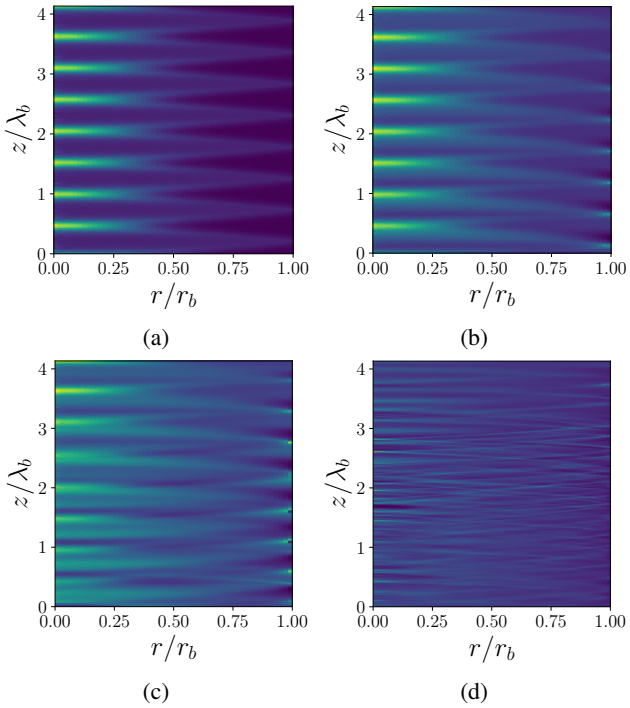

Figure 3: Particle number density $n(\tilde{r}, \tilde{z})$ for the KV $f_0(v)$ beam. (a) I = 0.0 mA (b) I = 0.1 mA (c) I = 0.5 mA (d) I = 5.0 mA

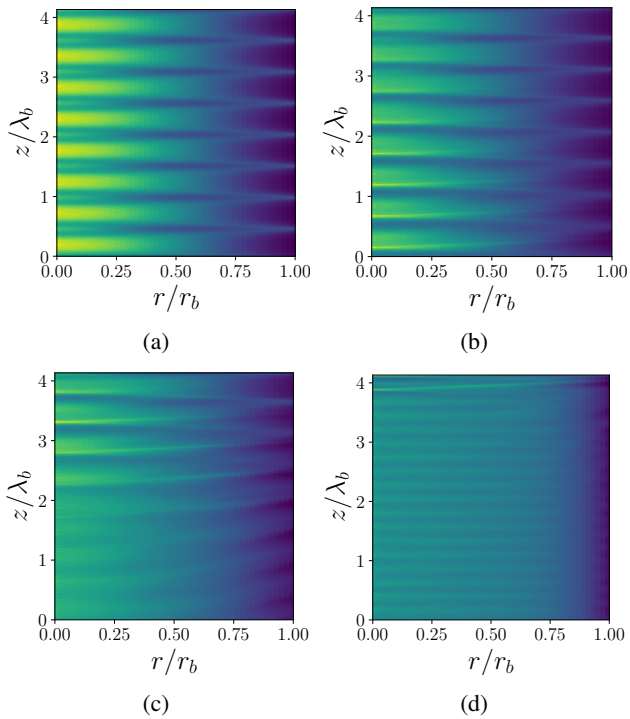

Figure 4: Particle number density $n(\tilde{r}, \tilde{z})$ for the PL $f_0(v)$ beam. (a) I = 0.0 mA (b) I = 0.1 mA (c) I = 0.5 mA (d) I = 5.0 mA

CONCLUSION

The mode spectrum excited by nonuniformity in configuration space leads to complex evolution of phase space dynamics influenced by initial velocity space distributions and space charge. Space charge accelerates beam evolution toward equilibrium commensurate with plasma period thermalization, while both PL and SG $f_0(v)$ suppress higher order mode correlations with the emittance. Further work is required to ascertain consistent tracking of the surface charge elements (not) corresponding to theory present within these beams and numerical integration near the beam edge. Future work will focus on changing the amount of the beam perturbation to observe how that influences modal dynamics and determining how and if these modes interact with each to produce complex dynamics.

ACKNOWLEDGEMENTS

This work has been supported by US DOE-HEP grants: DE-SC0010301 and DE-SC0022009.

ISBN: 978-3-95450-247-9 ISSN: 2673-5490 doi: 10.18429/JACoW-IPAC2024-MOPS82

REFERENCES

[1] L. A. Pocher, T. M. Antonsen, L. Dovlatyan, I. Haber, and P. G. O, "Optimizing the discovery of underlying nonlinear beam dynamics," in *Proc. NAPAC'22*, Albuquerque, NM, USA, 2022, pp. 335–338. doi:10.18429/JACoW-NAPAC2022-TUZE3

[2] L. Pocher, I. Haber, T. Antonsen, and P. O'Shea, "Optimizing the discovery of underlying nonlinear beam dynamics and moment evolution," in *Proc. IPAC'23*, Venice, Italy, May 2023, 2023, pp. 4503–4506. doi:10.18429/JACoW-IPAC2023-THPL036

[3] S. Nagaitsev *et al.*, "Accelerator and beam physics research goals and opportunities," 2021. doi:10.48550/arXiv:2101.04107

[4] B. M. de Silva, K. Champion, M. Quade, J.-C. Loiseau, J. N. Kutz, and S. L. Brunton, "PySINDy: A Python package for the sparse identification of nonlinear dynamics from data," *J. Open Source Software*, 2020. doi:10.48550/arXiv.joss.02104

[5] A. A. Kaptanoglu *et al.*, "PySINDy: A comprehensive Python package for robust sparse system identification," *J. Open Source Software*, vol. 7, p. 3994, 2022. doi:10.21105/joss.03994

[6] R. L. Gluckstern, "Oscillation modes in two dimensional beams," in *Proc. LINAC'70*, Batavia, IL, USA, Sep.-Oct. 1970, pp. 811–822. https://jacow.org/l70/papers/H-5.pdf

[7] S. M. Lund and R. C. Davidson, "Warm-fluid description of intense beam equilibrium and electrostatic stability properties," *Phys. Plasma*, vol. 5, no. 8, pp. 3028–3053, 1998. doi:10.1063/1.873027

[8] I. Hofmann, "Influence of the distribution function on eigenoscillations and stability of a beam," 1979.

[9] I. Hofmann, L. J. Laslett, L. Smith, and I. Haber, "Stability of the Kapchinskij-Kladimirskij (KV) distribution in long periodic transport systems," *Part. Accel.*, vol. 13, pp. 145–178, 1983.

[10] S. M. Lund, J. J. Barnard, and J. M. Miller, "On the relaxation of semi-gaussian and k-v beams to thermal equilibrium," in *Proc. PAC'95*, Dallas, TX, USA, May 1995, pp. 3278–3281.

[11] S. M. Lund, J. J. Barnard, and E. P. Lee, "Emittance growth for the thermalization of space-charged nonuniformities," Lawrence Berkelely National Laboratory, Tech. Rep., 2001.

[12] S. M. Lund, D. P. Grote, and R. C. Davidson, "Simulations of beam emittance growth from the collective relaxation of space-charge nonuniformities," *Nucl. Instrum. Methods Phys. Res. Sect. A*, vol. 544, no. 1, pp. 472–480, 2005. doi:10.1016/j.nima.2005.01.280

[13] B. E. Carlsten, "Thermalization of an intense, space-charge-dominated electron beam in a long focusing channel," *Phys. Rev. E*, vol. 60, no. 2, p. 2280, 1999. doi:10.1103/PhysRevE.60.2280

[14] E. Fermi, P. Pasta, S. Ulam, and M. Tsingou, "Studies of the nonlinear problems," Los Alamos National Lab.(LANL), Los Alamos, NM (United States), Tech. Rep. LA-1940, 1955. doi:10.2172/4376203

[15] D. P. Grote, A. Friedman, J.-L. Vay, and I. Haber, "The WARP code: Modeling high intensity ion beams," *AIP Conf. Proc.*, vol. 749, no. 1, pp. 55–58, 2005. doi:10.1063/1.1893366

[16] M. Reiser, *Theory and Design of Charged Particle Beams*. John Wiley & Sons: Hoboken, NJ, USA, 2008.